Revsbech, N. P., and Ward, D. M. (1984). Microelectrode studies of interstitial water chemistry and photosynthetic activity in a hot spring microbial mat. *Appl. Environ. Microbiol.* **48,** 270–275.

Schmitt-Wagner, D., and Brune, A. (1999). Hydrogen profiles and localization of methanogenic activities in the highly compartmentalized hindgut of soil-feeding higher termites (*Cubitermes* spp.). *Appl. Environ. Microbiol.* **65,** 4490–4496.

Schulz, H. N., and de Beer, D. (2002). Uptake rates of oxygen and sulfide measured with individual *Thiomargarita namibiensis* cells by using microelectrodes. *Appl. Environ. Microbiol.* **68,** 5746–5749.

Severinghaus, J., and Bradley, A. F. (1958). Electrodes for blood pO_2 and pCO_2 determination. *J. Appl. Physiol.* **13,** 515–520.

Further Readings

Damgaard, L. R., and Revsbech, N. P. (1997). A microscale biosensor for methane. *Anal. Chem.* **69,** 2262–2267.

Witty, J. F. (1991). Microelectrode measurements of hydrogen concentrations and gradients in legume nodules. *J. Exp. Bot.* **42,** 20–36.

[10] Optical Microsensors for Analysis of Microbial Communities

By MICHAEL KÜHL

Abstract

Fiber-optic microprobes connected to sensitive light meters are ideal tools to resolve the steep gradients of light intensity and spectral composition that prevail in aggregates and surface-associated microbial communities in sediments, biofilms, and microbial mats. They allow for a detailed mapping of light fields and enable insights to the complex optical properties of such highly light-scattering and -absorbing microbial systems. Used in combination with microsensors for chemical species, fiber-optic irradiance microprobes allow for detailed studies of photosynthesis regulation and of the photobiology of microbial phototrophs in intact samples under ambient microenvironmental conditions of the natural habitat. Fiber-optic microprobes connected to sensitive fluorometers enable microscale fluorescence measurements, which can be used to map (i) diffusivity and flow; (ii) distribution of photosynthetic microbes, via their photopigment autofluorescence; and (iii) activity of oxygenic photosynthesis via variable chlorophyll fluorescence measurements. Furthermore, by immobilizing optical indicator dyes on the end of optical fibers, fiber-optic

METHODS IN ENZYMOLOGY, VOL. 397 0076-6879/05 $35.00

DOI: 10.1016/S0076-6879(05)97010-9

microsensors for temperature, salinity, and chemical species such as oxygen, pH, and CO_2 can be realized.

Introduction

Niels Peter Revsbech introduced electrochemical microsensors to microbial ecology in the 1970s. Numerous applications (e.g., reviewed in Revsbech and Jørgensen, 1986) and the introduction of new types of microsensors (reviewed in Kühl and Revsbech, 2001) have since revolutionized our understanding of microenvironments and microenvironmental controls in microbial communities. However, not all relevant environmental variables can be measured with electrochemical measuring principles. Fiber-optic microsensors measure characteristics of the light field (e.g., irradiance or fluorescence) in front of the fiber tip (so-called microprobes) or quantify the amount of an analyte in the tip surroundings via a change in the optical properties of an indicator dye immobilized onto the fiber tip (so-called microoptodes). Fiber-optic microsensors take advantage of the inherent light-guiding capability of optical fibers. The light-collecting and guiding properties of optical fibers depend on the fiber materials used. Light is guided through the central core of the fiber via internal reflection at the core-cladding interface caused by a slightly higher refractive index in the core than in the surrounding cladding material. Both glass fibers and plastic fibers are suitable for sensor fabrication, but plastic fibers show a higher attenuation of ultraviolet (UV) and blue light and are more difficult to cut flat or taper in a controlled way (but see Merchant *et al.*, 1999). For applications involving light guiding of UV radiation, fused silica fibers with a high amount of OH^- are preferable, whereas fibers for VIS-NIR applications have a low amount of OH^- groups in the glass material. Both single mode and multimode fibers can be used for making fiber-optic microsensors. However, the very small core diameter of single mode fibers makes optical alignment difficult and efficient light transmission is best achieved with coherent laser radiation.

The microsensors mentioned in this chapter are all based on multimode optical fibers. There are many good sources for optical fibers, but some companies, such as Polymicro Technologies, USA, and Ceramoptec, Germany, focus on many specialized types of glass fibers, which are excellent for sensor fabrication. This chapter gives an overview of fiber-optic microsensors, which have been applied in environmental microbiology or which have a large potential for application in this field. The development and application of these sensors in microbiology are still limited to a few groups and most examples given in this chapter are from the author's own work. However, microoptodes for oxygen and pH are now

available commercially and are used more frequently in environmental studies.

General Construction Procedures for Simple Fiber-Optic Microprobes

Basic Properties and Handling of Optical Fibers

Simple glass fiber-optic microprobes that exhibit defined directional light-emitting or light-collecting properties can be constructed easily from commercially available optical fiber cables, so-called patch cords, that come mounted with standardized fiber connectors; an excellent and more detailed introduction to the construction and characterization of fiber-optic microprobes is given in Vogelmann *et al.* (1991). The simplest microprobe consists of a single-strand multimode fiber-optical cable with the light-collecting end of the optical fiber exposed and flat cut. Such a fiber accepts light within a narrow field of view around its longitudinal axis as given by the acceptance angle:

$$\Theta_a = \sin^{-1}(NA) \tag{1}$$

where the numerical aperture, $NA = \sqrt{(n_1^2 - n_2^2)}/n_0$, is defined by the refractive index of the fiber core, n_1, of the surrounding cladding material, n_2, and of the surrounding medium, n_0, respectively. The acceptance angle gives the maximal angle of incident light, which will be guided by internal reflection through the optical fiber. Note that the acceptance angle of optical fibers varies with the refractive index of the medium surrounding the fiber tip, n_0. Thus, a fiber microprobe with a given acceptance angle in air ($n_0 = 1$) will have a smaller acceptance angle when its tip is immersed in water ($n_0 \sim 1.33$). Typically, such microprobes range from 50 to 200 μm in diameter, depending on which fiber type is used. The construction is as follows (Holst *et al.*, 2000; Kühl and Jørgensen, 1992).

First the protective coating is removed from the fiber cable, exposing the bare optical fiber over a length of ~5–7 cm; this can be done easily with commercial fiber-stripping tools. The fiber end is cut flat with a commercial fiber-cleaving tool and the exposed fiber is then carefully inserted through and fixed (with fast-curing epoxy resin or UV-curing adhesive) in a hypodermic needle, which is mounted on a 1-ml plastic or glass syringe with the plunger removed (Fig. 1A). Alternatively, the fiber end can be cut after fixation in the needle by use of a diamond knife. Best support is obtained with a needle gauge that fits the fiber diameter closely. Fixation can be done with fast-curing epoxy resin or UV-curing glue. The latter is faster and causes no sliding of the fiber during the curing process.

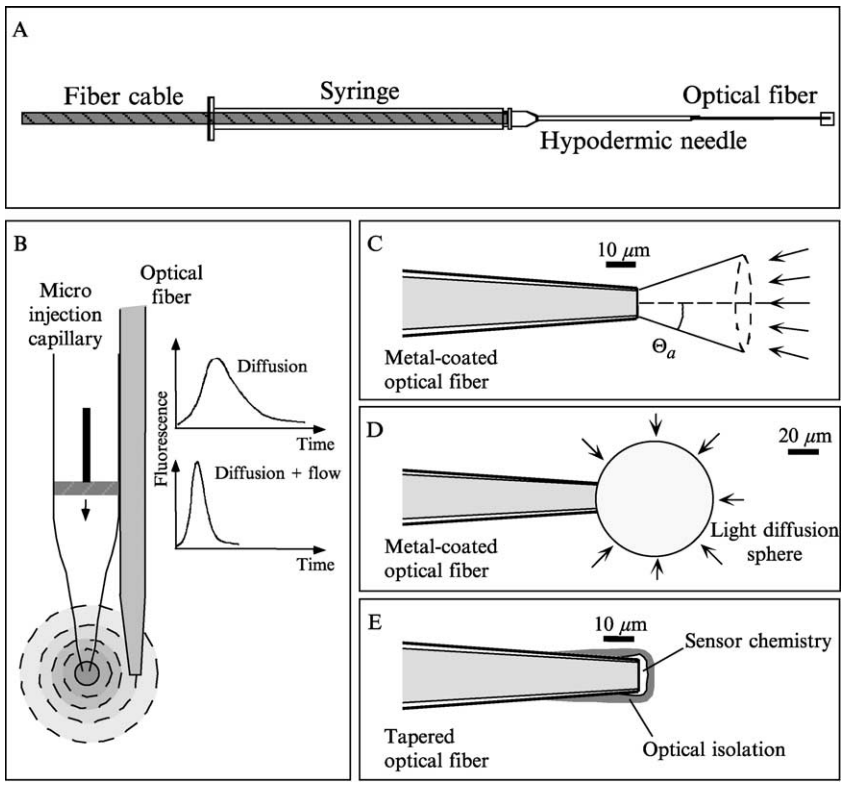

FIG. 1. Overview of different types of fiber-optic microsensors used in environmental microbiology. (A) Schematic drawing of how single-strand fibers can be fixed in a syringe that can be mounted on a micromanipulator. (B) A combined microinjection–microfluorescence sensor for optical measurement of diffusivity and flow. The capillary injects a small plume of a fluorescent dye, the concentration dynamics of which (small curves beside the sensor) is determined with a tapered optical fiber fixed at a known distance to the injection point. (C) Simple tapered fiber-optic microprobe, which is coated on the tapered sides with a metal coating. Such microprobes can be used for field radiance measurements or for microscale fluorescence measurements. (D) A scalar irradiance microprobe consisting of a small light-scattering sphere fixed onto the end of a tapered microprobe. The probe has an isotropic response to incoming light and is used to quantify the total radiative flux in light-scattering media. (E) A microoptode consisting of a tapered microprobe with a layer of optical indicator chemistry immobilized onto the tip (and, in some cases, with an additional optical isolation over the indicator layer). The indicator changes absorbance or luminescence as a function of an analyte in the tip surroundings. From Kühl and Revsbech (2001), with permission of the publisher.

Tapering Optical Fibers and Shaping of the Tapered Tip

By tapering the fiber tip, fiber-optic microprobes with tip diameters of <5 μm can be made. Most sensors are made of fused silica fibers, which soften at high temperatures. Tapering can be done in a small acetylene-oxygen or propane-oxygen flame; the author has had good experience with a hobby welding kit (Rothenberger GmbH, Germany). Alternatively, tapering of fibers can be done in an electric arc, as described in Grunwald and Holst (2004). With advanced (and expensive) laser pullers, even submicrometer tip diameters can be made reproducibly. A simple tapering procedure is as follows.

The syringe and needle with the mounted fiber are mounted vertically in a micromanipulator, with the fiber kept straight by a small weight. While observing it under a dissection scope, the fiber is carefully advanced toward the small flame until it softens and is stretched by gravity due to the attached weight. Slow softening and use of less weight make slender tapers, whereas shorter and faster softening and a heavier pulling weight make more conical tapers. Microprobes with short conical tapers exhibit best light transmission to/from the measuring tip and such geometry is advantageous for microscale fluorescence measurements and construction of microoptodes (Kohls *et al.*, 1998). After tapering, the fiber tip is cut flat at an appropriate diameter with a diamond knife or a commercial ceramic fiber-scratching tool. With some training, it is also possible to make a perfect flat cut fiber tip by careful scratching and breaking of the fiber with a sharpened watch-makers forceps while observing the fiber tip on a compound microscope at $10\times$ magnification.

Tapered fiber tips show a narrow light acceptance/emission angle, which is, however, masked by light coupling across the tapered sides of the tip. To avoid this leakage of light, the fiber tip can be coated with an optical isolation such as black enamel paint. The most durable isolation is, however, obtained by applying a metal coating on the fiber taper (Grunwald and Holst, 2004; Vogelmann *et al.*, 1991) (Fig. 1C). Careful heating of the tapered fiber tip in a small flame results in a widening of the acceptance angle. For this, the fiber tip is positioned toward the flame from below while inspected under a dissection microscope. As the fiber tip approaches the flame, the glass softens and forms a rounded tip on the taper. Fiber-optic microprobes with rounded tips show wider acceptance/emission angles than flat cut microprobes with the same diameter and taper geometry. Microprobes with a rounded tip are well suited for optimizing the spatial resolution of microscale fluorescence measurements with microprobes (see later).

Optoelectronic Detection Systems, Positioning, and Data Acquisition

Initially, the fabrication and use of fiber-optic microsensors relied on rather special materials and custom-made equipment, but the extremely rapid development in telecommunications and photonics has since enabled the use of standardized and readily available optical components and materials for sensor fabrication. The same holds true for the required optoelectronic detection systems. The author's initial work with fiber-optic microprobes in the late 1980s was done with a sensitive state-of-the-art diode array system that required water cooling and constant nitrogen flushing and filled a complete laboratory bench (Kühl and Jørgensen, 1992). In recent years, similar sensitivity has been approached with pocket-sized CCD-based spectrometers that can be run directly with a portable PC. The development of high-intensity LEDs (e.g., Luxeon, USA, and Nichia, Japan) and small photomultiplier modules (e.g., Hamamatsu Photonics, Japan/USA) has been another crucial development that has driven the development of fiber-optic microfluorometers. A detailed overview of optoelectronical instrumentation and components used with fiber-optic microsensors is not within the scope of this chapter but can be found in, for example, Holst *et al.* (2000).

Two types of light meters are commonly used with fiber-optic microsensors in environmental microbiology. An integral measurement of light over a certain wavelength range is done with sensitive photomultiplier tubes in combination with optical filters or a monochromator. Such systems have been developed for measuring photosynthetically active radiation for oxygenic photosynthesis (400–700 nm) (Kühl *et al.*, 1997) or for measuring fluorescence intensity or lifetime with fiber-optic microsensors (Holst *et al.*, 2000; Klimant *et al.*, 1995a,b; Thar *et al.*, 2001). Spectral light measurements are done with sensitive diode array or CCD-based fiber-optic spectrometers. Several fiber-optic spectrometers with suitable sensitivity for UV-NIR radiation (and a relatively low price) are now available commercially (e.g., PMA-11 from Hamamatsu Photonics, USA/Japan, the MMS-series from Carl Zeiss GmbH, Germany, and the USB2000 and QE65000 systems from Ocean Optics, USA).

The positioning of fiber-optic microsensors is done by help of a micromanipulator. The most common model used is a MM33 from Märzhäuser GmbH (Wetzlar, Germany). This is a manually operated micromanipulator, but it can be motorized and interfaced to a computer in various ways. A complete package for motorized positioning and simultaneous data acquisition with microsensors is available from Unisense A/S, Denmark. The system, which allows for autonomous profiling, is developed for use with electrochemical microsensors but is also very useful for measurements

with fiber-optic microsensors. Data acquisition (but no positioning control) is also provided with the microoptode-sensing systems from Presens GmbH, Germany.

Special measuring platforms, so-called benthic landers for autonomous *in situ* profiling with microoptodes in sediments, have also been developed for use at water depths up to 6000 m (e.g., Glud *et al.*, 1999a; Wenzhöfer *et al.*, 2001a,b), but none of these are currently available commercially.

Fiber-Optic Microsensors and Their Application

Surface Detection

A general problem when working with microsensors is to align measurements with the surface of the system investigated, e.g., the sediment or biofilm surface. While this can often be accomplished in the laboratory by visual inspection of the sample surface with a dissection microscope, very heterogeneous samples or measurements *in situ* request other methods for surface detection. Optical surface detection is possible by use of a tapered optical fiber connected to a simple modulated light meter equipped with a beam-splitting device (Klimant *et al.*, 1997a). Near-infrared radiation is emitted from the fiber tip, and the reflected NIR radiation from it is collected and guided to a photodiode via the same fiber-optic microprobe. As the microprobe approaches the sediment/biofilm surface, an increasing amount of backscattered radiation is coupled into the fiber tip (Fig. 2A). When the microprobe tip touches the sediment/biofilm interface, the largest increase in backscattered radiation is detected, which can be used to define the surface. With fiber tip diameters of 20–30 μm, the spatial resolution of the optical surface detection is better than 50 μm. When the microprobe tip is fixed to the tip of other microsensors, optical surface detection can be combined easily, e.g., with microscale oxygen measurements (Fig. 2B).

Fiber-Optic Diffusion and Flow Sensors

The mass transfer properties of surface-associated microbial communities are major determinants of microbial activity and zonations. Knowledge about diffusive and advective transport in sediments and biofilms is thus crucial for a quantitative interpretation of microsensor data, e.g., calculations of solute fluxes and reaction rates from concentration microprofiles. Electrochemical microsensors for flow and diffusivity have been developed (see Kühl and Revsbech, 2001), and other techniques, such as high-resolution nuclear magnetic resonance imaging approaches, have

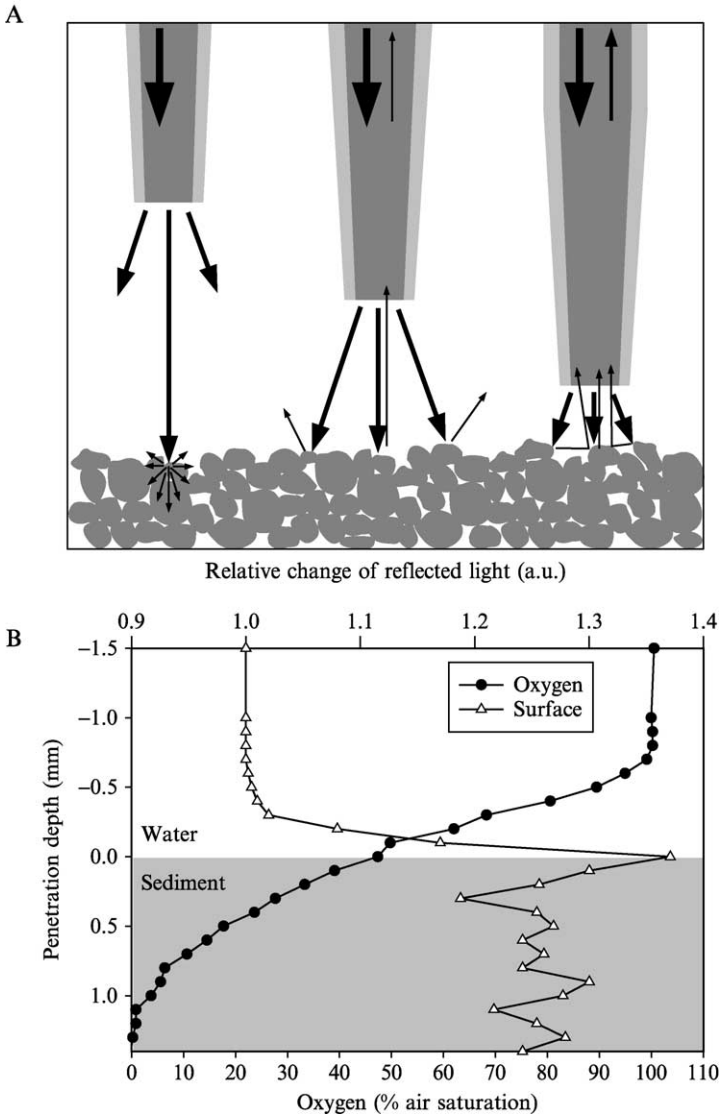

FIG. 2. (A) Principle of optical surface detection with a fiber-optic microprobe. Modulated NIR light is emitted from the fiber tip and is backscattered from the surface. As the microprobe tip approaches the interface, an increasing amount of backscattered light is collected by the microprobe. At the interface the largest relative change in reflectance is measured. (B) Combined microprofiling and surface detection with oxygen microsensors glued together with a fiber-optic microprobe at the measuring tip. After Klimant *et al.* (1997) and Holst *et al.* (2000), with permission of the publishers.

been used to map diffusivity in microbial mats at high spatial resolution (e.g., Wieland *et al.*, 2001). An optical approach for measuring diffusivity and flow was developed by DeBeer (1997) by combining a glass capillary microinjection system with a fiber-optic microprobe connected to a microfluorometer (Fig. 1B).

After injection of a small (picoliter) volume of a fluorescent dye, the plume will equilibrate with the surroundings at a rate that depends on the diffusive and advective transport properties in the matrix. The dye concentration in front of the fiber-optic microprobe tip, which is quantified via the dye fluorescence, will vary over time as the plume is equilibrating. The concentration field of the dye can be described as a function of time by (pg. 29 in Crank, 1975):

$$C = \frac{1}{2} C_0 \cdot \left[erf\left(\frac{a+r}{2\sqrt{Dt}}\right) + erf\left(\frac{a-r}{2\sqrt{Dt}}\right)\right] - \frac{C_0}{r}\sqrt{\frac{Dt}{\pi}} \cdot \left[e^{\left(-(a-r)^2/4Dt\right)} - e^{\left(-(a+r)^2/4Dt\right)}\right] \quad (2)$$

where t is elapsed time, r is the radius of the plume, a is the initial radius, and C_0 is the initial dye concentration in the injected plume; *erf()* is the error function. The local dye concentration, C, is approximated by the fluorescence intensity measured by the microprobe. If the distance between the point of injection and the fiber tip is known and the time between injection and fluorescence detection is determined precisely, then the diffusion coefficient, D, can be obtained by iterative fitting of the time-dependent fluorescence signal with Eq. (2). Furthermore, once the diffusion coefficient of the dye has been determined by measuring in stagnant conditions, Eq. (2) can be used to quantify flow velocity, v, by replacing r with $(r + vt)$.

This combined approach has been used to describe the transition from advective transport in the outer layers of biofilms to pure diffusive transport in the biofilm interior (De Beer, 1997). The properties of the fluorochrome are critical for the method. The dye solution must have the same viscosity and density as the liquid in the sediment porewater or biofilm, and the dye must not exhibit strong surface binding or change fluorescence in response to porewater chemistry. In some systems, clogging of the microinjection capillary is a problem.

Fiber-Optic Refractive Index Microsensor

The refractive index is a key factor affecting the optical properties of sediments and biofilms (Kühl and Jørgensen, 1994). The presence of microbial exopolymers with a slightly higher refractive index than water can

especially affect the light propagation and it is speculated that this is a key mechanism causing light-trapping effects in the surface layers of sediments and biofilms (Decho *et al.*, 2003; Kühl and Jørgensen, 1994). However, a detailed investigation of the refractive index in surface-associated microbial communities is still missing.

By coating tapered fiber-optic microprobe tips completely with thin metal layers, microsensors for refractive index measurements have been developed (Grunwald and Holst, 2004). The sensing principle is based on the surface plasmon resonance effect: White light sent to the fiber tip causes electron waves (surface plasma waves) at the interface between the metal layer and the surrounding medium that resonate with the incident light, causing a characteristic spectral minimum in the light that is guided back from the fiber tip to a spectral detector. The resonance, and therefore the value of the spectral minimum, is strongly dependent on the refractive index of the medium in immediate contact with the metal-coated fiber tip. Such sensors can be calibrated in commercially available solutions with a precisely known refractive index (e.g., from Cargille Labs, USA; www.cargille.com).

The sensors can be used for measurements of refractive indices from 1.300 to 1.380 at an accuracy of $\sim$0.001 and at a spatial resolution of about 100 μm (Grunwald and Holst, 2004). Examination of the tissues of ascidians containing symbiotic cyanobacteria indeed showed a higher refractive index in the gelatinous test material, where light trapping was observed (Kühl and Larkum, 2002), as compared to the overlaying seawater. With these new sensors it should now be possible to perform the first detailed studies of refractive index in microbial exopolymers, which are often providing the embedding matrix of microbial communities. Such measurements will be important for advancing our understanding of the optical properties of surface-associated microbial communities (Kühl and Jørgensen, 1994).

Fiber-Optic Microprobes for Mapping Light Fields

Surface-associated microbial communities in biofilms and sediments exhibit a strong attenuation of light due to absorption and intense scattering in the matrix of pigmented cells, exopolymers, and mineral grains. The first microscale light measurements in the environment started with the pioneering work of Vogelmann (e.g., Vogelmann and Bjørn, 1984; Vogelmann, 1991) and Jørgensen (e.g., Jørgensen and Des Marais, 1986, 1988), who used tapered fibers to map light fields in plant tissue and microbial mats, respectively. Their work was inspired by developments in biomedical optics, where researchers had developed and used similar techniques for studying the optical properties of animal tissue in connection with

photodynamic cancer therapy (reviewed in Star, 1997). Previous reviews of microscale light measurements in environmental microbiology can be found in Jørgensen (1989) and Kühl *et al.* (1994a). A comprehensive introduction to the optics of sediments and biofilms as measured with fiber-optic microprobes is given by Kühl and Jørgensen (1994). Figure 3 gives an overview of central optical parameters relevant for characterizing light fields in microbial communities. Each of the parameters can be measured by a fiber-optic microprobe as described in the following.

Field-Radiance Microprobes. Simple tapered and flat cut fiber microprobes (Fig. 1C) have a narrow acceptance angle for light and thus are ideal tools for mapping the field radiance, $L(\theta, \phi)$, i.e., the incident quantum flux per unit solid angle and area from a certain direction specified by the zenith (θ) and the azimuth (ϕ) angle in a spherical coordinate system. The field radiance is the fundamental parameter for describing the spatial light field and, depending on the actual measuring angle relative to the incident light, different components of the light field can be measured with field radiance

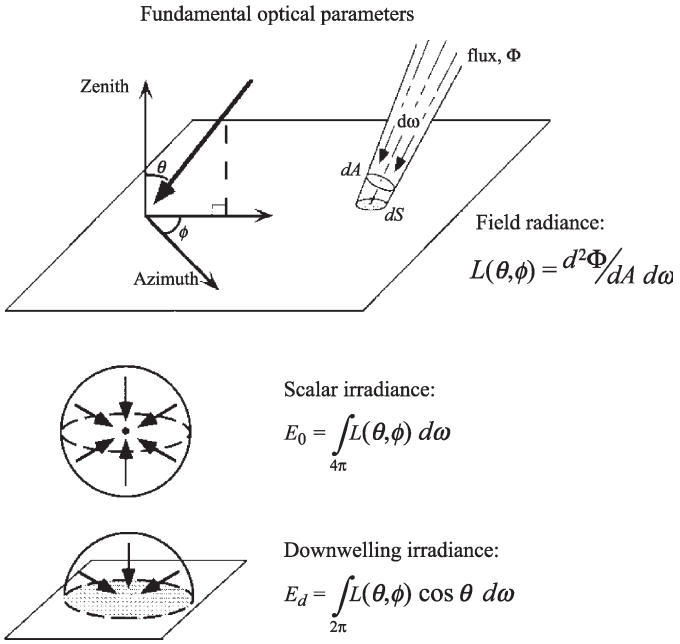

FIG. 3. The three basic optical parameters used to characterize light fields in environmental microbiology. Each of the parameters can be measured with a fiber-optic microprobe with light collection properties according to the definition of the parameter (see also Fig. 5). From Kühl and Jørgensen (1994), with permission of the publisher.

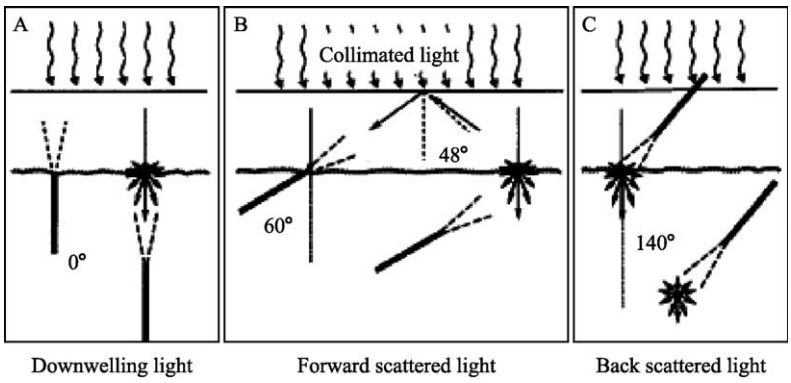

FIG. 4. Fiber-optic microprobes for field radiance measurements can be used to map various components of the light field, such as downwelling light (A), forward scattered light (B), and backscattered light (C) in microbial communities. From Kühl and Jørgensen (1994), with permission of the publisher.

microprobes (Fig. 4). Backscattered light is measured by approaching the biofilm or sediment sample from above, while downwelling and forward scattered light is measured by penetrating the sample from below. The latter requires the sample to be mounted in a core sealed at the bottom with a plug of agar or similar soft material that the microprobe can penetrate.

Numerous field radiance measurements in a sample under multiple different insertion angles allow a very detailed mapping of the light field from which a multitude of optical parameters and information on the radiative transfer can be derived after some mathematical treatment of data (Fukshansky-Kazarinova *et al.*, 1996, 1997, 1998; Kühl and Jørgensen, 1994). However, such measurements are time-consuming, and complete data sets can only be obtained in samples such as sediments and some microbial mats that do not exhibit structural changes over time due to migrating microbes (Kühl *et al.*, 1994a).

Spectral field radiance measurements of downwelling or backscattered light can be used to describe the zonation and migration of differently pigmented photosynthetic microbes at high spatial resolution (e.g., Jørgensen and Des Marais, 1986; Kühl *et al.*, 1994a; Bebout and Garcia-Pichel, 1995; Pringault and Garcia-Pichel, 2004) and have also been used to study the microscale distribution of special protective host pigments in symbiont-bearing corals (Salih *et al.*, 2000); such measurements complement similar studies based on microscale fluorescence measurements with tapered microprobes (see later). However, it is important to realize that

field radiance measurements only map the radiant flux from a narrow solid angle and therefore do not quantify the total amount of light available at a certain position in a microbial community.

Scalar Irradiance Microprobes. Optical studies with field radiance microprobes show that diffuse scattered light is a major source of energy for photosynthesis in biofilms and sediments (Jørgensen and Des Marais, 1988; Kühl and Jørgensen, 1994). Photosynthetic microbes in such systems harvest light from all directions, and it is most relevant to relate microbial photosynthesis at a given point to the total incident quantum flux from all directions, i.e., the spherical integral of the radiance distribution, which is the so-called quantum scalar irradiance,

$$E_0 = \int_{4\pi} L(\theta, \phi)$$

This parameter can be measured with a fiber-optic scalar irradiance microprobe consisting of a 80- to 100-μm-wide integrating sphere immobilized onto the tip of a 10- to 15-μm-wide tapered field radiance microprobe (Fig. 1D). Two fabrication methods have been described.

One method is based on dip coating the radiance microprobe in a viscous white mixture of methacrylate and titanium dioxide crystals (Lassen *et al.*, 1992a); best dispersion of the light-scattering particles in methacrylate is obtained with organically coated titanium dioxides often used in the painting industry. Due to the surface tension of the viscous material, a small droplet adhering to the fiber tip will tend to form a sphere, which solidifies as the solvent evaporates. Another method is based on tapering the fiber tip into a long thin filament, which is dipped in magnesium oxide and then melted back and shaped into a scattering vitro-ceramic spherical tip by careful heating in a small flame (Garcia-Pichel, 1995). The latter method allows construction of scalar irradiance microprobes for UV radiation. This is not possible with the dip-coating procedure, as UV is absorbed in the methacrylate matrix. With some training, both types of sensors can be made with an excellent isotropic response, i.e., light from all directions is channeled equally effectively by into the fiber and guided to the detector (Fig. 5). It is, however, crucial that the tapered sides of the fiber tip are coated with an optical isolation (see earlier discussion) in order to avoid nonideal light collection at oblique angles.

Scalar irradiance microprobes are easy to use, even in the field, as they can be positioned into the sample from above. The ''blind spot'' where the optical fiber connects with the integrating sphere only amounts to about 6% of the spherical surface area, and when inserted at a zenith angle of 135–145° relative to the incident light, self-shadowing is insignificant.

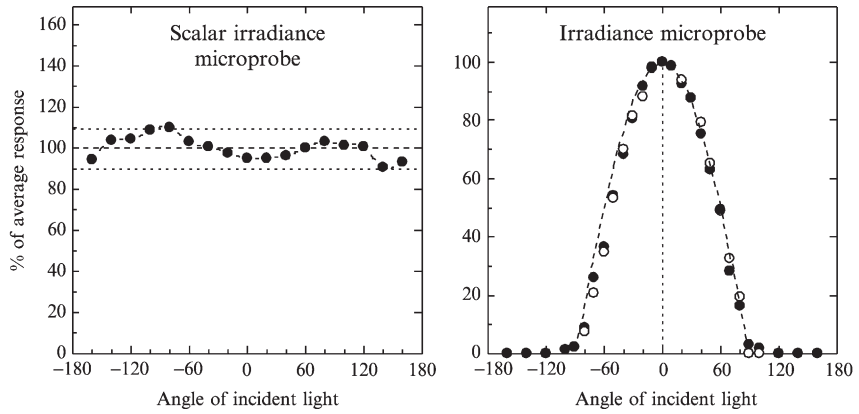

FIG. 5. Angular light collection properties of fiber-optic scalar irradiance and irradiance microprobes. The ideal angular response is indicated with dashed lines. From Kühl *et al.* (1994a), with permission of the publisher.

Scalar irradiance microprobes are relatively sturdy and can last for several years; they have been used in all kinds of systems, ranging from quartz sand to very cohesive microbial mats, plant, and animal tissues.

Calibration is often done by normalizing measurements obtained in a sample to measurements of the downwelling scalar irradiance (=downwelling irradiance in a collimated vertically incident light beam) measured with the microprobe tip positioned, at identical distance and orientation to the light source, over a black light well with minimal reflection of the downwelling light; a small petri dish or beaker coated with thick black velvet or with a matte black enamel paint has proven an excellent material for this. If the calibration is done with a calibrated lamp having a known absolute intensity for a given wavelength and distance from the light source, readings of the scalar irradiance microprobe can also be calibrated in absolute units of μmol photons m^{-2} s^{-1} (see, e.g., Kühl *et al.*, 1997).

Spectral attenuation coefficients of scalar irradiance, $K_0(\lambda)$, with depth, z, can be calculated as

$$K_0(\lambda) = -\frac{d \ln[E_0(\lambda)]}{dz} = -\frac{\ln[E_0(\lambda)_1 / E_0(\lambda)_2]}{z_2 - z_1} \tag{3}$$

where $E_0(\lambda)_1$ and $E_0(\lambda)_2$ are the spectral scalar irradiance measured at depths z_1 and z_2, respectively. Equation (3) can also be used to calculate attenuation coefficients of radiance and irradiance.

Scalar irradiance microprobes are ideal tools for optical studies in surface-associated communities (e.g., Kühl *et al.*, 1994a; Garcia-Pichel, 1995). In combination with oxygen microsensor measurements, detailed photobiological studies can be performed on intact samples, where regulation of microbial photosynthesis can be studied under natural conditions as a function of spectral composition or intensity (e.g., Ploug *et al.*, 1993; Lassen *et al.*, 1992b; Kühl *et al.*, 1996, 1998). The intensity and spectral characteristics of available light in different depths can be mapped and the presence of different photopigments can be determined (Fig. 6). Light availability in undisturbed samples can be precisely aligned with the distribution of oxygen and oxygenic photosynthesis (Fig. 7). This enables studies of how photosynthesis is regulated by light intensity in undisturbed samples with steep light gradients (Fig. 8), and spectral attenuation and photosynthetic action spectra can be determined for 0.1-mm-thin layers (Fig. 9). Probably the most surprising finding when scalar irradiance microprobes were first used in environmental microbiology studies was

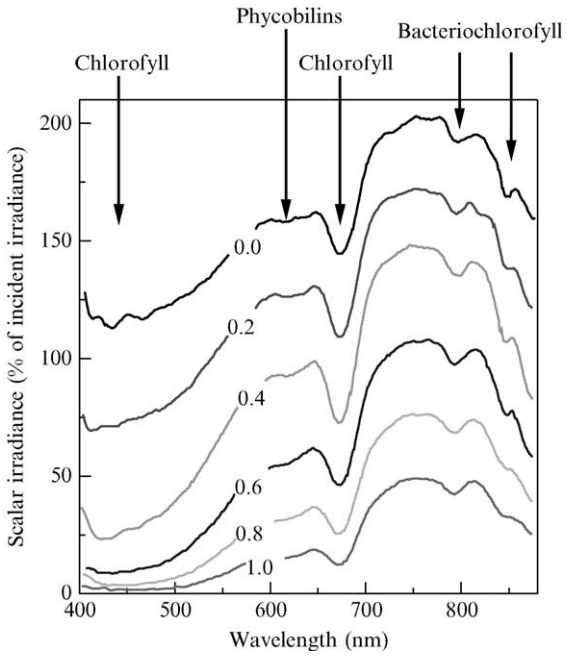

FIG. 6. Spectral measurements of scalar irradiance in a coastal sediment covered by a stratified microbial mat containing diatoms, cyanobacteria, and purple sulfur bacteria. Characteristic minima in the spectra correspond to absorption maxima of different photopigments as indicated with arrows.

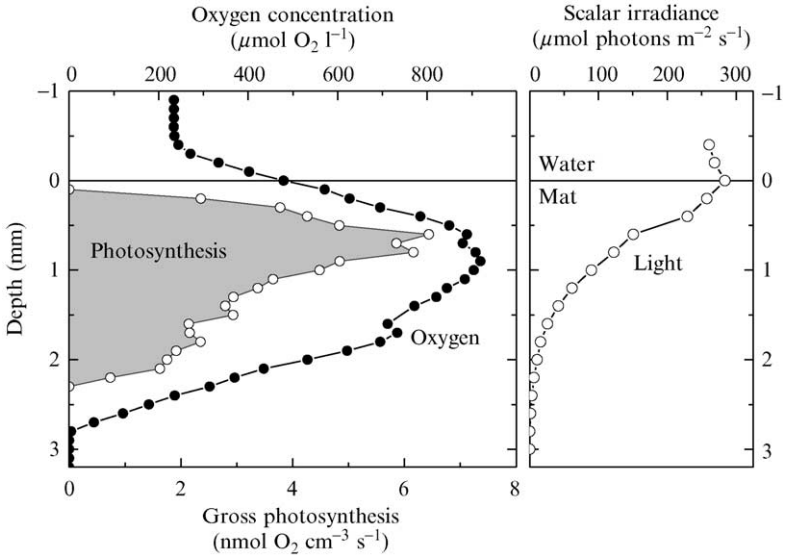

FIG. 7. Combined measurements of oxygen, oxygenic photosynthesis, and quantum scalar irradiance of photosynthetic active radiation (PAR, 400–700 nm) in a coastal sediment with a cyanobacterial mat. After Kühl *et al.* (1992), with permission of the publisher.

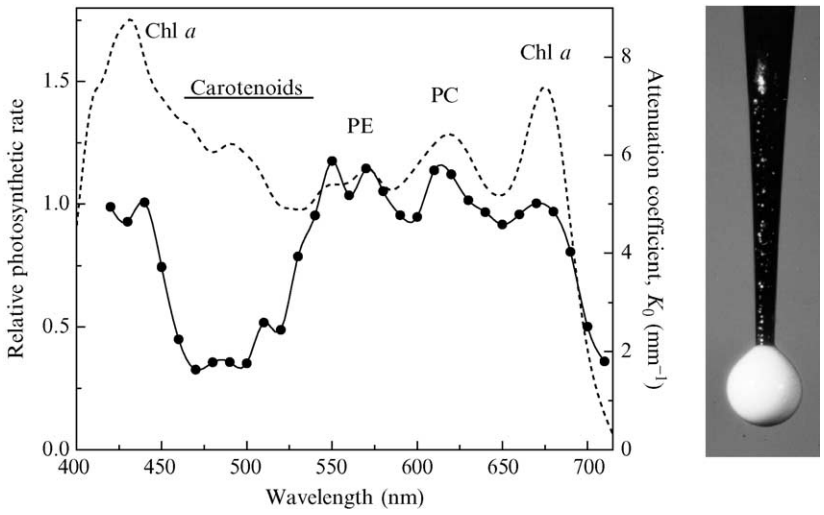

FIG. 8. Scalar irradiance attenuation spectrum (dashed line) and photosynthetic action spectrum (solid line) measured in the upper 0.1 mm of an intact epilithic cyanobacterial biofilm. The absorption regions of major photosynthetic pigments [chlorophyll *a*, phycocyanin (PC), and phycoerythrin (PE)] are indicated. After Kühl *et al.* (1996), with permission of the publisher.

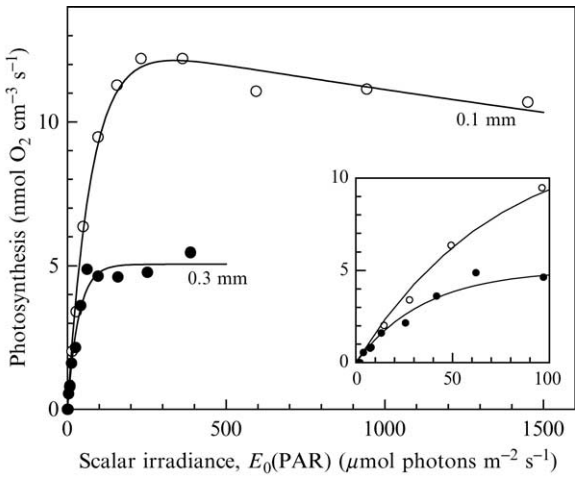

FIG. 9. Gross photosynthesis vs scalar irradiance measured at two different depths in a hypersaline cyaobacterial mat. The upper mat layer gets photoinhibited at high irradiance, while the strong light attenuation in the mat only results in saturation of photosynthesis at a 0.3-mm depth. After Kühl *et al.* (1997), with permission of the publisher.

that the scalar irradiance exhibits a surface or near-surface maximum (Kühl and Jørgensen, 1992, 1994; Lassen *et al.*, 1992) in many sediments and microbial mats (Figs. 6, 7, and 11). However, such light-trapping effects have also been observed in other scattering media and tissues (e.g., Vogelman and Björn, 1986) and the phenomenon is not a violation of thermodynamics but a consequence of photon statistics and path length distribution. Incident light is strongly scattered in the matrix of cells, mineral grains, and exopolymers, causing photons to travel an increased path length per vertical distance traversed. This increases the residence time of photons near the sediment/biofilm surface, which add onto incident photons and causes a local transient enhancement of scalar irradiance. The upper layers of strongly scattering sediments and mats thus act as a kind of ''bottleneck'' for photons on their way into deeper layers.

Irradiance Microprobes. The most commonly used quantification of light intensity in environmental microbiology is done in terms of the quantum irradiance, i.e., the integral quantum flux per unit horizontal surface area from above, i.e., the downwelling irradiance,

$$E_d = \int_{2\pi} L(\theta, \phi)\cos(\theta)$$

or from below, the upwelling irradiance, E_u. Note that the incident field radiance is weighted by the cosine of its zenith angle, and scattered light traveling at oblique angles is thus weighted less than vertically incident light. The ratio between upwelling and downwelling irradiance is called the irradiance reflectance,

$$R = E_u/E_d$$

which is a key parameter in remote-sensing studies of soils, sediment and mats. The difference between downwelling and upwelling irradiance is the vector irradiance, $\vec{E} = E_d - E_u$, which is a measure of the net radiant energy input to a system.

Irradiance microprobes with a good angular cosine response are difficult to make and have not found widespread application; a practical problem is also that microprofiling of downwelling irradiance requires penetration of the sample from below. The fabrication of irradiance microprobes involves the formation of a small light-scattering disk on the end of a tapered or untapered optical fiber, which is then coated on the sides with black enamel paint (Kühl *et al.*, 1994b; Lassen and Jørgensen, 1994). In practice, this is done by first applying a small droplet of methacrylate doped with TiO_2 (the same material used for making scalar irradiance microprobes) onto the fiber tip. After complete hardening, the white droplet is coated with black enamel paint. Subsequently, the now black droplet is carefully ground down with a small diamond drill bit to form a white disk surrounded by a black rim. With some training, such irradiance microprobes can be made with an almost ideal angular cosine response to incident light (Fig. 5).

As indicated earlier, neither microscale radiance nor irradiance measurements are sufficient for quantifying the available light for photosynthesis in sediments, biofilms, and other surface-associated microbial communities. However, the combined use of irradiance and scalar irradiance sensors is a strong tool for microscale determination of spectral absorption coefficients, $a(\lambda)$, in such intensely light-scattering systems by using Gershuns equation (Kühl and Jørgensen, 1994; Lassen and Jørgensen, 1994):

$$a(\lambda) = K_{\bar{E}}(\lambda).\frac{\vec{E}(\lambda)}{E_0(\lambda)} \tag{4}$$

where $K_{\bar{E}}$ is the vertical attenuation coefficient [see Eq. (3)] of the vector irradiance, $\vec{E}$, and E_0 is the scalar irradiance. Absorption coefficients are important for calculating quantum yields of photosynthesis.

Microscale Mapping of Pigment Fluorescence and Photosynthetic Activity

While microbial activity can be studied in great detail and almost noninvasively with microsensors, the distribution of microorganisms is mainly determined with various semidestructive microscopic techniques in combination with specific *in situ* hybridization or staining protocols (Amann and Kühl, 1998). The distribution of different photosynthetic microorganisms can, however, be detected and discriminated in intact samples by microscale mapping of their characteristic pigment fluorescence with a tapered fiber-optic microprobe (Kühl and Fenchel, 2000; Thar *et al.*, 2001) (Fig. 10). By fixing fiber-optic microprobes to the measuring tip of an oxygen microsensor, the distribution of oxygen and oxygenic photosynthesis can be mapped simultaneously with the distribution of chlorophyll (Fig. 11).

Using the same kind of microprobes with a more advanced pulse–amplitude-modulated fluorescence detector system (Schreiber *et al.*, 1996), the photosynthetic activity of microbes with oxygenic photosynthesis can be mapped. This method relies on measurements of variable

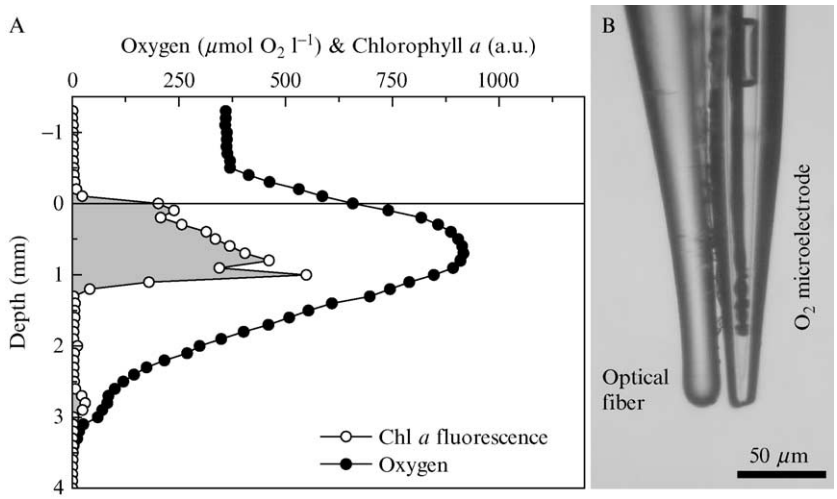

FIG. 10. Combined measurements of oxygen and chlorophyll *a* fluorescence (A) with a Clark-type oxygen microsensor glued together with the tapered tip of a fiber-optic microprobe (combined diameter ~40 μm, B). Measurements were done at a temperature of 0.5° and a downwelling irradiance of 130 μmol photons m^{-2} s^{-1} in an Arctic sediment covered with a dense biofilm of benthic diatoms (Young Sound, northeast Greenland) (Kühl *et al.,* unpublished data).

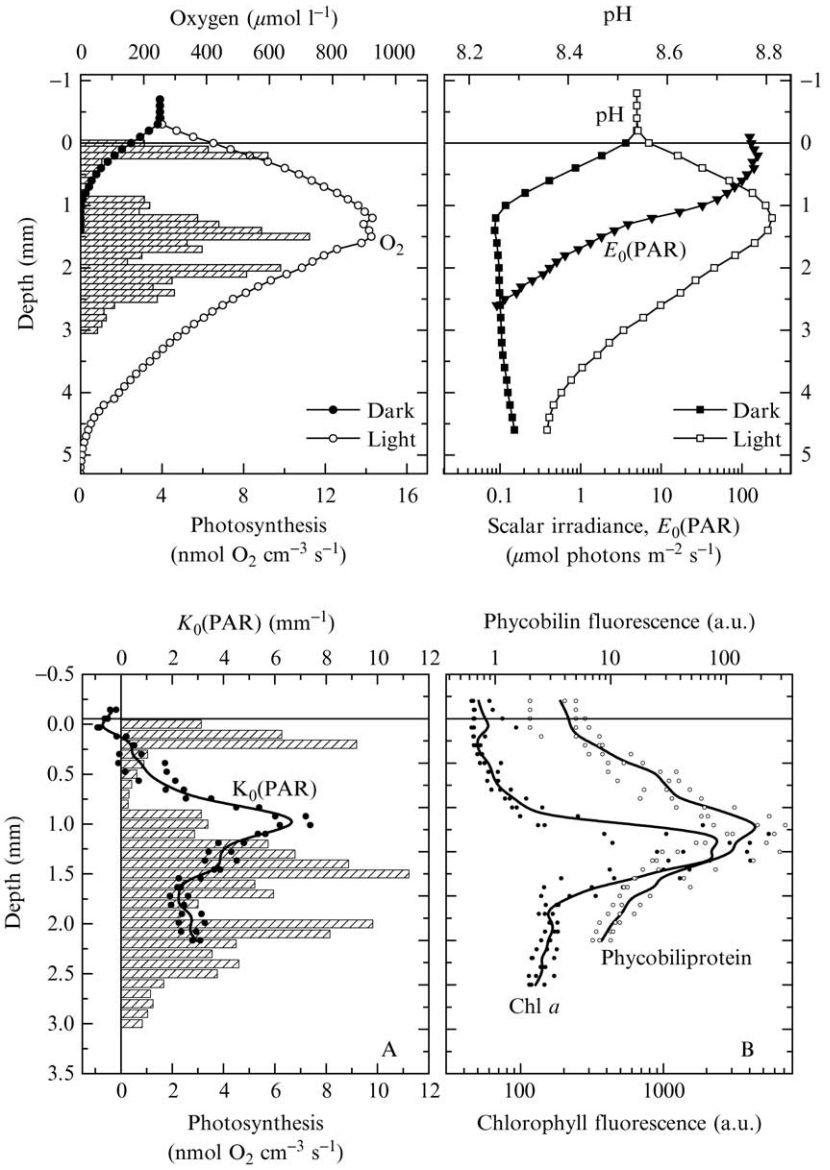

FIG. 11. Combined measurements of oxygen, pH, oxygenic photosynthesis, scalar irradiance (top), light attenuation, and photopigment fluorescence (bottom) in a cyanobacterial mat. From Kühl and Fenchel (2000), with permission of the publisher.

chlorophyll fluorescence from PSII in oxygenic phototrophs with the so-called saturation-pulse method (Schreiber, 2004). The method, which is not described in detail here, allows the determination of the effective quantum yield of PSII-related electron transport, ϕ_{II} (in units of mole electrons transported per mole quanta causing charge separation in PSII), from measurements of the chlorophyll fluorescence yield under ambient light, F, and during an intense saturation pulse that fully closes the reaction center, F_m':

$$\phi_{II} = \frac{F_m' - F}{F_m'} \tag{5}$$

When the sample is fully dark adapted, Eq. (3) is used to calculate the maximal PSII quantum yield, $\phi_{II(max)}$, from the minimal fluorescence signal in the dark, F_0, and the maximum fluorescence yield in the saturation pulse, F_m. As the actinic light intensity increases, the reaction center approaches full closure and the effective quantum yield decreases. Relative rates of the photosynthetic activity (in terms of a relative electron transport rate, $rETR$) can be estimated as $rETR = \phi_{II} \cdot E_0$, where E_0 is the scalar irradiance of actinic light.

Much more information on the status and function of the photosynthetic apparatus can be obtained from variable chlorophyll fluorescence measurements [a comprehensive treatment is given in Papageorgiou and Govindjee (2004)]. A simple measure of the nonphotosynthetic energy dissipation, i.e., the nonphotochemical quenching, NPQ, can be calculated as

$$NPQ = \frac{F_m - F_m'}{F_m'} \tag{6}$$

Variable fluorescence measurements are rapid, and measurements of rETR and energy dissipation as a function of different irradiances can be obtained repeatedly over time scales ranging from seconds to hours, allowing for detailed studies of photoacclimation and photoinhibition. The first microscale measurements of variable chlorophyll fluorescence were done in terrestrial leafs at a spatial resolution of 20–30 μm with a custom-made detection system (Schreiber *et al.*, 1996). A commercial version is now available (Microfiber-PAM, Walz GmbH, Germany), and this system has been used to map photosynthesis in sediments, biofilms, and corals (Ralph *et al.*, 2002). A combined microsensor, where the tip of a microfiber probe is fixed to the measuring tip of an oxygen microsensor (Fig. 10A), can be used to obtain both oxygen- and fluorescence-based measurements of

photosynthesis at ~100-μm spatial resolution. Combined measurements variable chlorophyll fluorescence and oxygen with fiber-optic of microsensors (see later) were used to study the oxygen regulation of photosynthesis in a cyanobacterial mat (Schreiber *et al.*, 2002). Variable chlorophyll fluorescence-imaging systems have been developed and applied for studying photosynthesis at similar high spatiotemporal resolution in various surface-associated microbial communities (e.g., Grunwald and Kühl, 2004; Kühl *et al.*, 2005; Ralph *et al.*, 2005).

Microoptodes

Microoptodes are tapered fiber-optic microsensors with one or more optical indicators immobilized at the measuring tip of the fiber (Holst *et al.*, 2000; Klimant *et al.*, 1997) (Fig. 1E). The indicator (also called the sensor chemistry) changes its optical properties (e.g., absorbance or fluorescence) reversibly as a function of the local level of the analyte to be measured. Miniature optical chemosensors were first developed for blood-gas analysis in the biomedical field, and the basic-sensing principles (see, e.g., Wolfbeis, 1991, 2003) have largely been adopted and optimized in the development of microoptodes for use in environmental microbiology. This section focuses mainly on microoptodes for oxygen, which are now applied frequently in various fields of environmental microbiology. In addition, it comments briefly on microoptodes for pH, CO_2, and temperature and their potential for application in environmental microbiology. Several types of microoptodes are available commercially (see, e.g., the Web pages of Presense GmbH, World Precision Instruments Inc., and Ocean Optics Inc.).

Oxygen Microoptodes

OPTICAL SENSING OF OXYGEN AND CALIBRATION. Oxygen can be measured optically by different luminescent indicator dyes that exhibit a dynamic quenching of their luminescence intensity, I, and life-time (=decay time), τ, for a given oxygen concentration, c, according to the well-known Stern–Volmer relation (Wolfbeis, 1991, 2003):

$$\frac{I}{I_0} = \frac{\tau}{\tau_0} = \frac{1}{1 + K_{SV} \cdot c} \tag{7}$$

where I_0 and τ_0 are the luminescence intensity and life-time, respectively, of the indicator in the absence of oxygen, and K_{SV} is a characteristic quenching coefficient of the indicator. Energy from excited dye molecules is transferred to molecular oxygen, whereby singlet oxygen is formed, which is rapidly relaxing under emission of heat. Note that oxygen optodes exhibit the highest signal and signal changes at low oxygen concentrations.

When indicators are immobilized in a matrix material, their luminescence as a function of oxygen often exhibits a nonideal Stern–Volmer behavior, which can be described by the modified relation (Klimant *et al.*, 1995a,b) (Fig. 12):

$$\frac{I}{I_0} = \frac{\tau}{\tau_0} = \frac{1-\alpha}{1+K_{SV}\cdot c} + \alpha \tag{8}$$

where α is a nonquenchable fraction of the indicator luminescence. The oxygen concentration, c, can thus be expressed as

$$c = \frac{(I_0 - I)}{K_{SV}\cdot(I - I_0\alpha)} = \frac{(\tau_0 - \tau)}{K_{SV}\cdot(\tau - \tau_0\alpha)} \tag{9}$$

For a given mixture of indicator and matrix material, α is usually constant over the dynamic range, and Eq. (8) accurately describes the nonlinear behavior of I or τ vs oxygen concentration (Fig. 12). α can be determined from measurements of luminescence from at least three defined oxygen concentrations (e.g. 0, $c_1 = 20\%$ oxygen saturation, and $c_2 = 100\%$ oxygen saturation) as follows (Glud *et al.*, 1996).

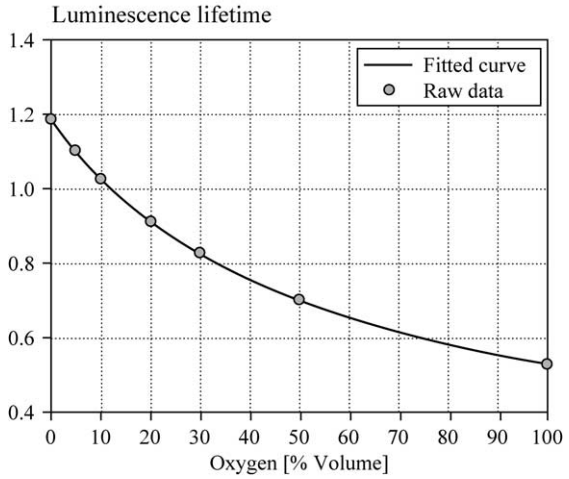

FIG. 12. Calibration curve of an oxygen microoptode based on the oxygen-dependent luminescence lifetime of an indicator dye immobilized at the end of a tapered microprobe. Solid symbols represent actual measurements, and the solid line was fitted to data with Eq. (8). From Holst *et al.* (2000), with permission of the publisher.

First the quenching constant, K_{SV}, can be determined as

$$K_{SV} = \frac{I_0(c_2 - c_1) - (I_1 c_2 - I_2 c_1)}{(I_1 - I_2) \cdot c_1 \cdot c_2} \tag{10}$$

The nonquenchable fraction, α, can then be determined as

$$\alpha = \frac{I_1(1 + K_{SV} c_1) - I_0}{I_0 \cdot K_{SV} \cdot c_1} \tag{11}$$

Once α has been determined, calibration of optical oxygen sensors can thus be done by a simple two-point calibration, i.e., measurements at zero oxygen and at a known oxygen concentration. In many aquatic applications of oxygen microsensors, a reading for zero oxygen is reached when profiling into deeper layers of sediments and biofilms, and a reading in the overlaying water can be related to the oxygen content determined by a Winkler titration or from tables of oxygen solubility in water if the medium is air-flushed and has a known temperature and salinity (such tables can be downloaded freely from *www.unisense.com* and *www.presense.de*). If a zero oxygen reading is not reached in the measurement, a zero oxygen calibration point can be measured by immersing the microoptode tip into a small subsample of the overlaying water made anoxic by the addition of small amounts of sodium dithionite.

FABRICATION OF OXYGEN MICROOPTODES. The first oxygen microoptodes were developed by Klimant *et al.* (1995) and have since found increasing application in various fields of environmental microbiology. Oxygen microoptodes are made from tapered fiber-optic microprobes (see earlier discussion), where the sensing tip is coated with an optical indicator dissolved in a hydrophobic and oxygen-permeable immobilization matrix (Fig. 1E) [see Holst *et al.* (2000) for more details on microoptode construction]. A small droplet of this so-called sensor cocktail is applied to the tip of the microprobe and will form a solid sensor layer after the solvent is evaporated. The thin sensor layer does not absorb all excitation light, which can lead to local stimulation of oxygen production when microoptodes are used for measurements in dense photosynthetic samples such as planktonic aggregates or biofilms and microbial mats. Also, strong intrinsic fluorescence in the sample, e.g., high chlorophyll concentrations, can interfere with the measurements. In order to avoid such effects, the sensor layer is coated (by dip coating) with a thin black layer of an oxygen-permeable optical isolation, i.e., black silicone or a black solution of the Teflon AF polymer (Dupont, USA).

The operational range and sensitivity of oxygen microoptodes can be optimized by the choice of indicator type and immobilization matrix. Two types of indicator material are used commonly for oxygen microoptodes: metalloorganic complexes of ruthenium(II) (excited by blue light and emitting orange light) (Klimant *et al.*, 1995, 1999) and porphyrines with platinum or palladium as the central atom (excited by UV or blue-green light and emitting red or NIR light) (Papkovsky, 2004). Tris(4,7-diphenyl-1,10-phenantroline)-ruthenium(II) (RuDPP) is the most frequently used ruthenium-based indicator dye with oxygen microoptodes. RuDPP-based microoptodes exhibit very good photostability, as well as good and homogeneous sensitivity over a broad dynamic range from 0 to >500% air saturation. Porphyrine-based microoptodes have a more narrow dynamic range (platinum–porphyrines: 0–250%, and palladium-porphyrines: 0–~10% air saturation) but exhibit higher sensitivity (Fig. 13).

The oxygen solubility and permeability of the immobilization matrix also affect the sensitivity of oxygen microoptodes. For a given ambient oxygen level, a higher solubility results in a higher amount of quenching

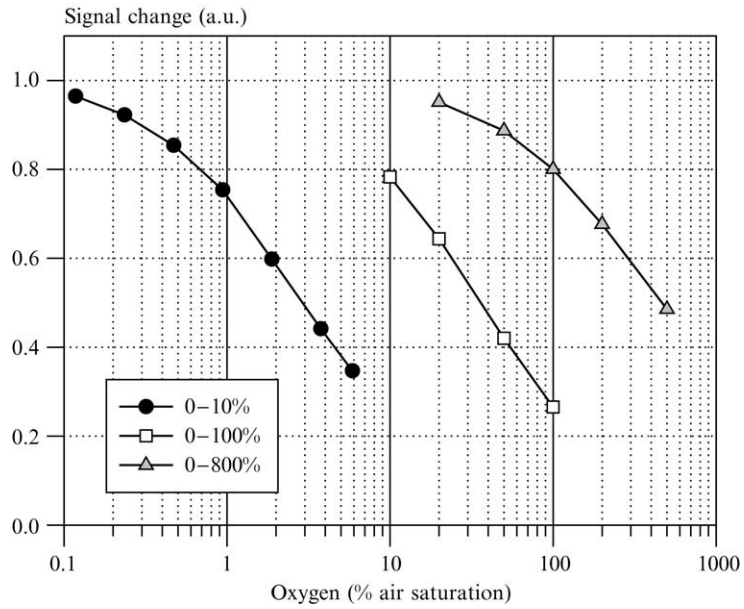

FIG. 13. Calibration curves of oxygen optodes made of three different materials: palladium–porphyrin (●), platinum–porphyrin (□), and ruthenium (△). The oxygen zero point of all curves is suppressed because of the logarithmic scale. From Holst *et al.* (2000), with permission of the publisher.

oxygen in the sensor layer, causing a higher signal change. In practice, the need for good mechanical stability of the matrix is limiting the choice of material. Although silicone has high oxygen solubility, it is not a good matrix for oxygen microoptodes, which are used for profiling in solid or semisolid substrates. Instead, polystyrene, which has significantly lower oxygen solubility, good mechanical stability and adhesion to the fiber glass, is often used for immobilizing the indicator layer to the fiber tip. Organically modified sol-gels (so-called *Ormosils*) can also be used as an immobilization matrix with oxygen microoptodes, and their oxygen permeability can be optimized by the proper choice of formation conditions and amounts of precursor material (Klimant *et al.*, 1999).

PERFORMANCE AND APPLICATION OF OXYGEN MICROOPTODES. First applications of oxygen microoptodes relied on the use of luminescence intensity-based measurements. However, intensity-based luminescence measurements are subject to interferences from ambient light, changes of the optical properties in the surroundings of the measuring tip, e.g., when entering from water into a scattering and/or fluorescent matrix, and microbending of the optical fiber, causing changes in light transmission. While most of these interferences can be overcome or minimized by coating the measuring tip with an optical isolation (see earlier discussion), they become irrelevant with luminescence lifetime-based measurements, which rely on time-dependent changes in signal, which are essentially independent on absolute signal intensity (as long as there is enough signal at all times) (Holst *et al.*, 2000).

Oxygen microoptodes and instrumentation for lifetime-based oxygen measurements are available commercially (from Presense GmbH, Germany), and since their development in 1995 they have been used in many different aquatic and terrestrial habitats and systems (e.g., Schreiber *et al.*, 2002; Mock *et al.*, 2002). For most applications in environmental microbiology oxygen microoptodes and microelectrodes are equally suitable and give identical results. However, for special applications needing a very fast response time ($<$0.5 s), such as measurements of gross photosynthesis with the light–dark shift method (see Revsbech and Jørgensen, 1986), oxygen microelectrodes remain the best alternative; oxygen microoptodes currently have response times down to about 1 s in aqueous media.

Oxygen microoptodes (and oxygen optodes in general) have no inherent oxygen consumption in contrast to oxygen microelectrodes that generate a current in proportion to the amount of oxygen consumed by the measuring cathode (see Kühl and Revsbech, 2001). Microoptodes therefore show the same signal in a solution kept at constant oxygen levels whether it is stagnant or not, whereas oxygen microelectrodes typically show a 1–3% lower signal under stagnant conditions (Klimant *et al.*,

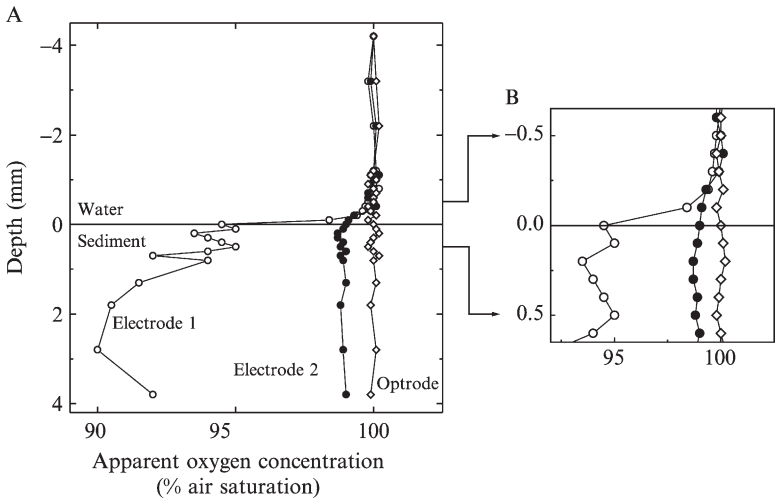

FIG. 14. Stirring sensitivity of microsensors can lead to artifacts when measuring oxygen microprofiles in surface-associated microbial communities. Microprofiles of apparent O_2 concentration in an artificial sediment with a stirred water phase above, as measured by an O_2 microoptode and Clark-type O_2 microelectrodes with a high (electrode 1) and a low (electrode 2) stirring sensitivity, respectively. There was no real gradient of O_2 present in the system. From Klimant *et al.* (1995), with permission of the publisher.

1995a; Fig. 14). Reduced gases such as hydrogen sulfide can poison oxygen microelectrodes, which is not the case with oxygen microoptodes.

By using porphyrine indicator dyes, oxygen microoptodes can be made with a very high sensitivity toward low oxygen concentrations (down to 1 ppb), where oxygen microelectrodes have a limited sensitivity. Another advantage of oxygen microoptodes in comparison to electrochemical oxygen microsensors is that they exhibit a relatively small-pressure dependency of the signal. This is an advantage for *in situ* applications where microoptodes are used for oxygen profiling in the deep sea (Glud *et al.*, 1999a; Wenzhöfer *et al.*, 2001a,b). Oxygen microoptodes are solid-state sensors, which perform well even at subzero temperatures, and have been used for oxygen measurements in sea ice (Mock *et al.*, 2002), where the sensors were frozen into the ice matrix during formation, and for profiling the sea ice–water interface (Mock *et al.*, 2003).

Other Microoptodes for Use in Environmental Microbiology. Several other types of microoptodes have been described (Wolfbeis, 2004), and several of these have found application in environmental microbiology. This section gives a brief account of the most relevant types. With the

accelerating development of optical sensor technology, the author foresees that many new types of microoptodes will be developed and will find increasing application in environmental microbiology. An interesting topic not touched upon in this chapter is the construction of fiber-optic biosensors (e.g., Marazuela and Moreno-Bondi, 2002; Wolfbeis, 2004), where enzymes, antibodies, fluorescent molecular beacons, or whole cells are immobilized onto fiber tips, where they induce an optical change when reacting (or binding) to a specific compound in the tip surroundings. The field is under rapid development, specifically the use of whole cells containing reporter gene fusions (Hansen and Sørensen, 2001), which will allow the construction of new types of fiber-optic microsensors for use in environmental microbiology.

TEMPERATURE MICROOPTODES. Luminescence dyes exhibit a temperature dependency, which can be used to fabricate temperature microoptodes. A simple way to accomplish this is to immobilize luminescent oxygen-sensitive dyes in a matrix impermeable of oxygen or, alternatively, to place an oxygen microoptode inside a sealed capillary (Holst *et al.*, 2000). Such temperature microoptodes exhibit a linear response of the luminescence lifetime vs temperature over a range from 0 to 45° and with a precision of about 0.1–0.2° (Klimant *et al.*, 1997). In comparison to microthermocouples, which are affected by heat conduction to or from the measuring tip via the wires when measuring in a temperature gradient, temperature microoptodes give a better spatial resolution, as heat conduction in the glass material is much less than in metal wires (Holst *et al.*, 1997b). Temperature microoptodes can be used to map steep temperature gradients in hot spring environments or for studying temperature dynamics in strongly absorbing microbial communities such as microbial mats (Klimant *et al.*, 1997).

pH MICROOPTODES. Like oxygen, pH is a key variable in most biological studies and many optical measuring schemes have been developed (see e.g., Wolfbeis, 1991), where pH is evaluated via a change in absorbance or fluorescence of a pH-sensitive indicator. Such optical pH sensors respond according to the mass acting law and do not show a log-linear response over a wide pH range such as potentiometric pH electrodes. Optical pH sensors thus have a limited dynamic range of approximately 3 to 4 pH units, i.e., $\pm$1.5–2 pH units around the pK value of the pH indicator. However, the resolution can be very high in the optimal range. While electromagnetic fields and sulfide or flow velocity effects on the reference electrode influence electrochemical pH measurement, the main interference on optical pH sensors is the ionic strength. However, this problem can be overcome using calibration buffers of similar ionic strength as the sample. Typically, calibration is performed in three to four buffer solutions covering the pH

range of the sensor. There are many different pH indicators available for optical sensors, but most indicators have a pK value toward the neutral or acidic range, whereas sensitive indicators with a pK around the pH of seawater are rare.

A simple pH microsensor was developed by Kohls *et al.* (1997) and was based on the immobilization of a commercial pH indicator (N9, Merck) in a sol-gel matrix onto the tip of a fiber-optic microprobe. The indicator changes absorbance as a function of pH, and this change is monitored by measuring the reflectance from the fiber tip when feeding two different wavelengths, i.e., light from a blue and a yellow LED, into the microfiber. The indicator exhibits a pK of ~8.2, and the pH microoptode exhibits a good accuracy of ±0.05 pH units over a range of pH 7–9 (the total useful range being pH 6.5–10). This microsensor thus covers the most relevant pH range for most applications in environmental microbiology.

Klimant and co-workers (2001; Kosch, 1999) have described a more advanced measuring scheme for pH based on fluorescent decay time measurements, and such pH microoptodes are now available commercially (from Presense GmbH). In these microsensors, the sensor chemistry consists of an inert long decay time reference dye and a short decay time indicator dye, which changes its fluorescence intensity due to the pH value. It can be shown (Klimant *et al.*, 2001) that the average decay time represents the ratio of the two fluorescence intensities. Therefore, the signal of such pH microoptodes is referenced internally and is thus insensitive to fluctuations of the light source. Commercial pH microoptodes have a dynamic range of pH 5.5–8.5 at a resolution of 0.01 pH units and with a response time <30 s.

CO_2 MICROOPTODES. Carbon dioxide levels in microbial communities are affected directly by autotrophic and heterotrophic microbes and indirectly by the interplay of microbial metabolism with the carbonate system in aquatic environments. In surface-associated communities, steep concentration gradients of CO_2 and pH exist and microscale measurements of CO_2 are thus highly relevant. Hitherto, electrochemical CO_2 microsensors have been applied mostly in environmental microbiology (e.g., DeBeer *et al.*, 1997, 2000; Köhler-Rink and Kühl, 2001), but *in situ* profiling with a CO_2 microoptode in the deep sea has been reported (Wenzhöfer *et al.*, 2002).

The latter study was done with a microoptode, which was based on the so-called Severinghaus principle (see Holst *et al.*, 2000), where CO_2 diffuses across a gas-permeable membrane into an internal buffer solution and induces a pH shift that can be monitored with a pH sensor. The microoptode consisted of a microcapillary (tip diameter 20 μm) sealed with a silicone plug and filled with a pH-sensitive luminescent dye (HPTS, Fluka).

The pH of the internal solution was monitored just behind the membrane by a tapered microprobe inserted into the outer casing and connected to a microfluorometer. Such CO_2 microoptodes have a response time of <2 min and a detection limit <5 μmol CO_2 liter^{-1}.

More recently, a CO_2 microoptode based on a tapered fiber coated with a nonaqueous hydrophobic CO_2-sensitive layer was described (Neurauter *et al.*, 2000). This sensor has a detection limit of <1 μmol CO_2 liter^{-1} and a response time <1 min. To our knowledge, this sensor has not yet been applied in environmental microbiology, although it has excellent measuring characteristics for studying the carbonate system in aquatic microbial communities.

Planar Optodes. An attractive feature of optical chemical sensors is the possibility of scaling up from microscale point measurements to simultaneous high-resolution imaging of larger areas by immobilizing the optical indicator on sensor foils instead of at the tip of an optical fiber. Using the same measuring and calibration principles, such sensor foils (so-called planar optodes) can be monitored with fluorescence intensity or lifetime imaging systems (e.g., Holst *et al*., 1998; Glud *et al*., 2001) for imaging two-dimensional oxygen (e.g., Glud *et al*., 1996, 1999b; König *et al*., 2001; Grunwald and Holst, 2001), pH (Hulth *et al*., 2002; Liebsch *et al*., 2000), and CO_2 (Liebsch *et al*., 2000) dynamics in microbial communities.

Acknowledgments

I thank colleagues, postdocs, and students with whom I have had the pleasure to develop and apply various fiber-optic microsensor techniques. I especially mention Bo Barker Jørgensen, Carsten Lassen, Ingo Klimant, and Gerhard Holst. The work has relied on the excellent technical assistance of Anni Glud. The Danish Natural Science Research Council, the Carlsberg Foundation (Denmark), the Max-Planck Society (Germany), and the European Commission (contracts: MAS3-CT-950029, MAS3-CT-970078, EVK3-CT-1999-00010, QLK3-CT-2002-01938) have strongly supported my own work with fiber-optic microsensors over the past 15 years.

References

Bebout, B., and Garcia-Pichel, F. (1995). UV B-induced vertical migrations of cyanobacteria in a microbial mat. *Appl. Environ. Microbiol.* **61,** 4215–4222.

Beyenal, H., Lewandowski, Z., Yakymyshyn, C., Lemley, B., and Wehri, J. (2000). Fiber-optic microsensors to measure backscattered light intensity in biofilms. *Appl. Opt.* **39,** 3408–3412.

Crank, J. (1975). ''The Mathematics of Diffusion,'' 2nd Ed. Oxford Univ. Press, New York.

De Beer, D. (1997). Microenvironments and mass transfer phenomena in biofilms and activated sludge studied with microsensors. *In* ''Proceedings of the International Symposium on Environmental Biotechnology'' (H. Verachtert and W. Verstraete, eds.), pp. 217–224. Koninklijke Vlaamse Ingenieurs Veriningng, Antwerpe.

Decho, A. W., Kawaguchi, T., Allison, M. A., Louchard, E., Reid, R. P., Stephens, C., Voss, K., Wheatcroft, R., and Taylor, B. B. (2003). Sediment properties influencing up-welling spectral reflectance signatures: The biofilm gel effect. *Limnol. Oceanogr.* **48,** 431–443.

Fukshansky-Kazarinova, N., Fukshansky, L., Kühl, M., and Jørgensen, B. B. (1996). Theory of equidistant three-dimensional radiance measurements with optical microprobes. *Appl. Opt.* **35,** 65–73.

Fukshansky-Kazarinova, N., Fukshansky, L., Kühl, M., and Jørgensen, B. B. (1997). General theory of three-dimensional radiance measurements with optical microprobes. *Appl. Opt.* **36,** 6520–6528.

Fukshansky-Kazarinova, N., Fukshansky, L., Kühl, M., and Jørgensen, B. B. (1998). Solution of the inverse problem of radiative transfer on the basis of measured internal fluxes. *J. Quant. Spectr. Rad. Trans.* **59,** 77–89.

Glud, R. N., Klimant, I., Holst, G., Kohls, O., Meyer, V., Kühl, M., and Gundersen, J. K. (1999a). Adaptation, test and *in-situ* measurements with O_2 microoptodes on benthic landers. *Deep-Sea Res. A* **46,** 171–183.

Glud, R. N., Kühl, M., Kohls, O., and Ramsing, N. B. (1999b). Heterogeneity of oxygen production and consumption in a photosynthetic microbial mat as studied by planar optodes. *J. Phycol.* **35,** 270–279.

Glud, R. N., Ramsing, N. B., Gundersen, J. K., and Klimant, I. (1996). Planar optrodes, a new tool for fine scale measurements of two dimensional O_2 distribution in benthic communities. *Mar. Ecol. Progr. Ser.* **140,** 217–226.

Glud, R. N., Tengberg, A., Kühl, M., Hall, P., Klimant, I., and Holst, G. (2001). An *in situ* instrument for planar O_2 optode measurements at benthic interfaces. *Limnol. Oceanogr.* **46,** 2073–2080.

Grunwald, B., and Kühl, M. (2004). A system for imaging variable chlorophyll fluorescence of aquatic phototrophs. *Ophelia* **58,** 79–89.

Grunwald, B., and Holst, G. (2004). Fibre optic refractive index microsensor based on white-light SPR excitation. *Sens. Act. A* **113,** 174–180.

Hansen, L. H., and Sørensen, S. J. (2001). The use of whole-cell biosensors to detect and quantify compounds or conditions affecting biological systems. *Microb. Ecol.* **42,** 483–494.

Holst, G., Klimant, I., Kohls, O., and Kühl, M. (2000). Optical microsensors and microprobes. *In* ''Chemical Sensors in Oceanography'' (M. Varney, ed.), pp. 143–188. Gordon & Breach.

Holst, G., Kohls, O., Klimant, I., König, B., Richter, T., and Kühl, M. (1998). A modular luminescence lifetime imaging system for mapping oxygen distribution in biological samples. *Sens. Act. B* **51,** 163–170.

Holst, G., Kühl, M., Klimant, I., Liebsch, G., and Kohls, O. (1997b). Characterization and application of temperature micro-optodes for use in aquatic biology. *SPIE Proc.* **2980,** 164–171.

Hulth, S., Aller, R. C., and Engstrom, P. (2002). A pH plate fluorosensor (optode) for early diagenetic studies of marine sediments. *Limnol. Oceanogr.* **47,** 212–220.

Jørgensen, B. B. (1989). Light penetration, absorption and action spectra in cyanobacterial mats. *In* ''Microbial Mats: Physiological Ecology of Benthic Microbial Communities'' (Y. Cohen and E. Rosenberg, eds.), pp. 123–137. *Am. Soc. Microbiol.*, Washington, DC.

Jørgensen, B. B., and Des Marais, D. J. (1986). A simple fiber-optic microprobe for high resolution light measurements: Application in marine sediment. *Limnol. Oceanogr.* **31,** 1376–1383.

Jørgensen, B. B., and Des Marais, D. J. (1988). Optical properties of benthic photosynthetic communities: Fiber-optic studies of cyanobacterial mats. *Limnol. Oceanogr.* **33,** 99–113.

Klimant, I., Holst, G., and Kühl, M. (1995b). Oxygen micro-optrodes and their application in aquatic environments. *SPIE Proc.* **2508,** 375–386.

Klimant, I., Holst, G., and Kühl, M. (1997). A simple fiber-optic sensor to detect the penetration of microsensors into sediments and other biological materials. *Limnol. Oceanogr.* **42,** 1638–1643.

Klimant, I., Huber, C., Liebsch, G., Neurauter, G., Stangelmayer, A., and Wolfbeis, O. S. (2001). Dual lifetime referencing (DLR): A new scheme for converting fluorescence intensity into a frequency-domain or time-domain information. *In* ''New Trends in Fluorescence Spectroscopy: Application to Chemical and Life Sciences'' (B. Valeur and J. C. Brochon, eds.), pp. 257–275. Springer Verlag, Berlin.

Klimant, I., Meyer, V., and Kühl, M. (1995a). Fiber-optic oxygen microsensors, a new tool in aquatic biology. *Limnol. Oceanogr.* **40,** 1159–1165.

Klimant, I., Ruckruh, F., Liebsch, G., Stangelmayer, A., and Wolfbeis, O. S. (1999). Fast response oxygen micro-optodes based on novel soluble ormosil glasses. *Mikrochim. Acta* **131,** 35–46.

Kohls, O., Holst, G., and Kühl, M. (1998). Micro-optodes: The role of fibre tip geometry for sensor performance. *SPIE Proc.* **3483,** 106–108.

Kohls, O., Klimant, I., Holst, G., and Kühl, M. (1997). Development and comparison of pH microoptodes for use in marine systems. *SPIE Proc.* **2978,** 82–94.

Köhler-Rink, S., and Kühl, M. (2001). Microsensor studies of photosynthesis and respiration in the larger foraminifera *Amphistegina lobifera* and *Amphisorus hemprichii*. *Ophelia* **55,** 111–122.

König, B., Holst, G., Kohls, O., Richter, T., Glud, R. N., and Kühl, M. (2001). Imaging of oxygen distribution at benthic interfaces: A brief review. *In* ''Organism-Sediment Interactions'' (J. Y. Aller, S. A. Woodin, and R. C. Aller, eds.), pp. 63–73. Univ. South Carolina Press, Columbia.

Kühl, M., Chen, M., Scheiber, U., Ralph, P. J., and Larkum, A. W. D. (2005). A niche for cyanobacteria with chlorophyll. *d. Nature* **433,** 820.

Kühl, M., and Fenchel, T. (2000). Bio-optical characteristics and the vertical distribution of photosynthetic pigments and photosynthesis in an artificial cyanobacterial mat. *Microb. Ecol.* **40,** 94–103.

Kühl, M., Glud, R. N., Ploug, H., and Ramsing, N. B. (1996). Microenvironmental control of photosynthesis and photosynthesis-coupled respiration in an epilithic cyanobacterial biofilm. *J. Phycol.* **32,** 799–812.

Kühl, M., and Jørgensen, B. B. (1992). Spectral light measurements in microbenthic phototrophic communities with a fiber-optic microprobe coupled to a sensitive diode array detector. *Limnol. Oceanogr.* **37,** 1813–1823.

Kühl, M., and Jørgensen, B. B. (1994). The light field of micro-benthic communities: Radiance distribution and microscale optics of sandy coastal sediments. *Limnol. Oceanogr.* **39,** 1368–1398.

Kühl, M., and Larkum, A. W. D. (2002). The microenvironment and photosynthetic performance of Prochloron sp. in symbiosis with didemnid ascidians. *In* ''Cellular Origin and Life in Extreme Habitats'' (J. Seckbach, ed.), Vol. 3, pp. 273–290. Kluwer, Dordrecht.

Kühl, M., Lassen, C., and Jørgensen, B. B. (1994a). Optical properties of microbial mats: Light measurements with fiber-optic microprobes. *In* ''Microbial Mats: Structure, Development and Environmental Significance'' (L. J. Stal and P. Caumette, eds.), pp. 149–167. Springer, Berlin.

Kühl, M., Lassen, C., and Jørgensen, B. B. (1994b). Light penetration and light intensity in sandy sediments measured with irradiance and scalar irradiance fiber-optic microprobes. *Mar. Ecol. Progr. Ser.* **105,** 139–148.

Kühl, M., Lassen, C., and Revsbech, N. P. (1997). A simple light meter for measurements of PAR (400–700 nm) with fiber-optic microprobes: Application for P vs. I measurements in microbenthic communities. *Aq. Microb. Ecol.* **13,** 197–207.

Lassen, C., and Jørgensen, B. B. (1994). A fiber-optic irradiance microsensor (cosine collector): Application for *in situ* measurements of absorption coefficients in sediments and microbial mats. *FEMS Microbiol. Ecol.* **15,** 321–336.

Lassen, C., Ploug, H., and Jørgensen, B. B. (1992a). A fibre-optic scalar irradiance microsensor: Application for spectral light measurements in sediments. *FEMS Microbiol. Ecol.* **86,** 247–254.

Lassen, C., Ploug, H., and Jørgensen, B. B. (1992b). Microalgal photosynthesis and spectral scalar irradiance in coastal marine sediments of Limfjorden, Denmark. *Limnol. Oceanogr.* **37,** 1813–1823.

Liebsch, G., Klimant, I., Frank, B., Holst, G., and Wolfbeis, O. S. (2000). Luminescence lifetime imaging of oxygen, pH, and carbon dioxide distribution using optical sensors. *Appl. Spectrosc.* **54,** 548–559.

Marazuela, M. D., and Moreno-Bondi, M. C. (2002). Fiber-optic biosensors: An overview. *Anal. Bioanal. Chem.* **372,** 664–682.

Merchant, D. F., Scully, P. J., and Schmitt, N. F. (1999). Chemical tapering of polymer optical fibre. *Sens. Act. A* **76,** 365–371.

Mock, T., Dieckmann, G., Haas, C., Krell, A., Tison, J. L., Belem, A., Papadimitriou, S., and Thomas, D. N. (2002). Micro-optodes in sea ice: A new approach to investigate oxygen dynamics during sea ice formation. *Aq. Microb. Ecol.* **29,** 297–306.

Mock, T., Kruse, M., and Dieckmann, G. (2003). A new microcosm to investigate the oxygen dynamics of the sea-ice water interface. *Aq. Microb. Ecol.* **30,** 197–205.

Neurauter, G., Klimant, I., and Wolfbeis, O. S. (2000). Fiber-optic microsensor for high-resolution pCO_2 sensing in marine environment. *Fresen. J. Anal. Chem.* **366,** 481–487.

Papageorgiou, G., and Govindjee, C. (2004). ''Chlorophyll Fluorescence: A Signature of Photosynthesis.'' Kluwer, Dordrecht.

Papkovsky, D. B. (2004). Methods in optical oxygen sensing: Protocols and critical analyses. *Methods Enzymol.* **383,** 715–734.

Ploug, H., Lassen, C., and Jørgensen, B. B. (1993). Action spectra of microalgal photosynthesis and depth distribution of spectral scalar irradiance in a coastal marine sediment of Limfjorden, Denmark. *FEMS Microbiol. Ecol.* **102,** 261–270.

Pringault, O., and Garcia-Pichel, F. (2004). Hydrotaxis of cyanobacteria in desert soils. *Microb. Ecol.* **47,** 366–373.

Ralph, P., Gademann, R., Larkum, A. W. D., and Kühl, M. (2002). Spatial heterogeneity in active fluorescence and PSII activity of coral tissues. *Mar. Biol.* **141,** 639–646.

Ralph, P. J., Schreiber, U., Gademann, R., Kühl, M., and Larkum, A. W. D. (2005). Coral photobiology studied with a new imaging PAM fluorometer. *J. Phycol.* **41,** 335–342.

Revsbech, N. P., and Jørgensen, B. B. (1986). Microelectrodes: Their use in microbial ecology. *Adv. Microb. Ecol.* **9,** 293–352.

Salih, A., Larkum, A. W. D., Cox, G., Kühl, M., and Hoegh-Guldberg, O. (2000). Fluorescent pigments in corals are photoprotective. *Nature* **408,** 850–853.

Schreiber, U. (2004). Pulse-amplitude-modulation (PAM) fluorometry and saturation pulse method: An overview. *In* ''Chlorophyll Fluorescence: A Signature of Photosynthesis'' (G. Papageorgiou and C. Govindjee, eds.), pp. 279–319. Kluwer, Dordrecht.

Schreiber, U., Gademann, R., Bird, P., Ralph, P., Larkum, A. W. D., and Kühl, M. (2002). Apparent light requirement for activation of photosynthesis upon rehydration of desiccated beachrock microbial mats. *J. Phycol.* **38,** 125–134.

Schreiber, U., Kühl, M., Klimant, I., and Reising, H. (1996). Measurement of chlorophyll fluorescence within leaves using a modified PAM fluorometer with a fiber-optic microprobe. *Photosynth. Res.* **47,** 103–109.

Star, W. M. (1997). Light dosimetry *in vivo*. *Phys. Med. Biol.* **42,** 763–787.

Thar, R., Kühl, M., and Holst, G. (2001). A fiber-optic fluorometer for microscale mapping of photosynthetic pigments in microbial communities. *Appl. Environ. Microbiol.* **67,** 2823–2828.

Vogelmann, T. C., and Björn, L. O. (1984). Measurements of light gradients and spectral regime in plant tissue with a fibre optic probe. *Photochem. Photobiol.* **41,** 569–576.

Vogelmann, T. C., Martin, G., Chen, G., and Buttry, D. (1991). Fibre optic microprobes and measurement of the light microenvironment within plant tissues. *Adv. Bot. Res.* **18,** 256–295.

Wenzhöfer, F., Adler, M., Kohls, O., Hensen, C., Strotmann, B., Boehme, S., and Schulz, H. D. (2001b). Calcite dissolution driven by benthic mineralization in the deep-sea: *In situ* measurements of Ca^{2+}, pH, pCO_2 and O_2. Geochim. *Cosmochim. Acta* **65,** 2677–2690.

Wenzhöfer, F., Holby, O., and Kohls, O. (2001a). Deep penetrating benthic oxygen profiles measured *in situ* by oxygen optodes. *Deep Sea Res. A* **48,** 1741–1755.

Wieland, A., van Dusschoten, D., Damgaard, L. R., de Beer, D., Kühl, M., and Van As, H. (2001). Fine-scale measurement of diffusivity in a microbial mat with NMR imaging. *Limnol. Oceanogr.* **46,** 248–259.

Wolfbeis, O. S. (1991). ''Fiber Optic Chemical Sensors and Biosensors.'' CRC Press, Boca Raton, FL.

Wolfbeis, O. S. (2003). A review on milestones in opt(r)ode technology unitil the year 2000. *In* ''Optical Sensors for Industrial, Environmental and Clinical Applications'' (R. Narayanaswamy and O. S. Wolfbeis, eds.), pp. 1–34. Springer, Berlin.

Wolfbeis, O. S. (2004). Fiber optic chemical sensors and biosensors. *Anal. Chem.* **76,** 3269–3283.

Further Readings

Amman, R., and Kühl, M. (1998). *In situ* methods for assessment of microorganisms and their activities. *Curr. Opin. Microbiol.* **1,** 352–358.

De Beer, D., Glud, A., Epping, E., and Kühl, M. (1997). A fast responding CO_2 microelectrode for profiling in sediments, microbial mats and biofilms. *Limnol. Oceanogr.* **42,** 1590–1600.

De Beer, D., Kühl, M., Stambler, N., and Vaki, L. (2000). A microsensor study of light enhanced Ca^{2+} uptake and photosynthesis in the reef-building coral *Favia* sp. *Mar. Ecol. Progr. Ser.* **194,** 75–85.

Holst, G., Glud, R. N., Kühl, M., and Klimant, I. (1997a). A microoptode array for fine scale measurements of oxygen distribution. *Sens. Act. B* **38–39,** 122–129.

Holst, G., Kühl, M., and Klimant, I. (1995). A novel measuring system for oxygen microoptodes based on a phase modulation technique. *SPIE Proc.* **2508,** 387–398.

Klimant, I., Kühl, M., Glud, R. N., and Holst, G. (1997b). Optical measurement of oxygen and temperature in microscale: Strategies and biological applications. *Sens. Act. B* **38,** 29–37.

Kosch, U., Klimant, I., Werner, T., and Wolfbeis, O. S. (1998). Strategies to design pH optodes with luminescence decay times in the μsecond time regime. *Anal. Chem.* **362,** 73–78.

Kühl, M., Fenchel, T., and Kazmierczak, J. (2003). Growth, structure and calcification potential of an artificial cyanobacterial mat. *In* ''Fossil and Recent Biofilms, a Natural History of Life on Earth'' (W. E. Krumbein, D. Paterson, and G. Zavarzin, eds.), pp. 77–102. Kluwer, Dordrecht.

Vogelmann, T. C., and Björn, L. O. (1986). Plants as light traps. *Physiol. Plant.* **68,** 704–708.